Acta Geochim
https://doi.org/10.1007/s11631-019-00367-5

ORIGINAL ARTICLE

The mixing of multi-source fluids in the Wusihe Zn–Pb ore deposit in Sichuan Province, Southwestern China

Hongjie Zhang[1,2] · Haifeng Fan[1] · Chaoyi Xiao[1,2] · Hanjie Wen[1,2] · Lin Ye[1] · Zhilong Huang[1] · Jiaxi Zhou[3] · Qingjun Guo[4]

Received: 5 April 2019 / Revised: 2 July 2019 / Accepted: 30 July 2019

Abstract The Sichuan–Yunnan–Guizhou (SYG) metallogenic province of southwest China is one of the most important Zn–Pb ore zones in China, with ~ 200 Mt Zn–Pb ores at mean grades of 10 wt.% Zn and 5 wt.% Pb. The source and mechanism of the regional Zn–Pb mineralization remain controversial despite many investigations that have been conducted. The Wusihe Zn–Pb deposit is a representative large-scale Zn–Pb deposit in the northern SYG, which mainly occurs in the Dengying Formation and yields Zn–Pb resources of ~ 3.7 Mt. In this paper, Zn and S isotopes, and Fe and Cd contents of sphalerite from the Wusihe deposit were investigated in an attempt to constrain the controls on Zn and S isotopic variations, the potential sources of ore-forming components, and the possible mineralization mechanisms. Both the δ^{66}Zn and δ^{34}S values in sphalerite from the Wusihe deposit increase systematically from the bottom to the top of the strata-bound orebodies. Such spatial evolution in δ^{66}Zn and δ^{34}S values of sphalerite can be attributed to isotopic Rayleigh fractionation during sphalerite precipitation with temperature variations. The strong correlations between the Zn–S isotopic compositions and Fe–Cd concentrations in sphalerite suggest that their variations were dominated by a similar mechanism. However, the Rayleigh fractionation mechanism cannot explain the spatial variations of Fe and Cd concentrations of sphalerite in this deposit. It is noted that the bottom and top sphalerites from the strata-bound orebodies document contrasting Zn and S isotopic compositions which correspond to the Zn and S isotopic characteristics of basement rocks and host rocks, respectively. Therefore, the mixing of two-source fluids with distinct Zn–S isotopic signatures was responsible for the spatial variations of Zn–S isotopic compositions of sphalerite from the Wusihe deposit. The fluids from basement rocks are characterized by relatively lighter Zn (~ 0.2 ‰) and S (~ 5 ‰) isotopic compositions while the fluids from host rocks are marked by relatively heavier Zn (~ 0.6 ‰) and S (~ 15 ‰) isotopic compositions.

Keywords Sichuan–Yunnan–Guizhou · Wusihe Zn–Pb deposit · Zn–S isotopes · Fe–Cd contents · Two-source fluids

1 Introduction

The Sichuan–Yunnan–Guizhou (SYG) metallogenic province is an important component of the giant South China low-temperature metallogenic domain (Hu et al. 2017). More than 400 carbonate-hosted Zn–Pb deposits occur in the SYG, yielding total Zn–Pb ores of more than 200 million tonnes at mean grades of 10 wt.% Zn and 5 wt.% Pb (Liu and Lin 1999; Zhou et al. 2014a, b). The sources for the regional Zn–Pb mineralization in the SYG remain controversial despite many investigations that have been conducted, mostly in regard to the Emeishan basalts, folded

✉ Haifeng Fan
fanhaifeng@mail.gyig.ac.cn

1 State Key Laboratory of Ore Deposit Geochemistry, Institute of Geochemistry, Chinese Academy of Sciences, Guiyang 550081, China

2 University of Chinese Academy of Sciences, Beijing 100049, China

3 School of Resource Environment and Earth Sciences, Yunnan University, Kunming 650504, China

4 Center for Environmental Remediation, Institute of Geographic Sciences and Natural Resources Research, Chinese Academy of Sciences, Beijing 100101, China

Published online: 10 August 2019

basements, and host rocks (Huang et al. 2003; Han et al. 2007; Ye et al. 2011; Zhou et al. 2014b, 2018; Zhu et al. 2016; Xiong et al. 2018). Most deposits in the SYG have been suggested to be comparable to Mississippi Valley-type (MVT), including many large-scale Zn–Pb deposits (e.g., the Huize, Daliangzi, Tianbaoshan, and Maozu deposits) (Han et al. 2007; Zhou et al. 2013; He et al. 2016; Wang et al. 2016). Otherwise, many deposits (e.g., the Wusihe deposit) distributed in the northern SYG are characterized by well strata-bound orebodies within the Dengying Formation and produce total Zn–Pb resources of $\sim$ 10 Mt (Xiong et al. 2018). The characteristics with well strata-bound orebodies of these deposits led them previously to be regarded as sedimentary exhalative (SEDEX) deposits (Lin 2005; Zhu et al. 2018). New evidence, however, shows that the Wusihe deposit could also be an MVT deposit based on detailed ore geology and geochemical data (Rb–Sr isochron age of 411 $\pm$ 10 Ma; Xiong et al. 2018).

Spatial variations of Zn isotopic in hydrothermal system have been well studied with three alternative interpretations, including temperature variation (Mason et al. 2005; Toutain et al. 2008; Pašava et al. 2014), Rayleigh fractionation (Wilkinson et al. 2005; Kelley et al. 2009; Gagnevin et al. 2012; Zhou et al. 2014a, b; Gao et al. 2017), and mixing of multi-source fluids (Wilkinson et al. 2005). Among the above three mechanisms, fluid mixing has not yet been fully understood because it is difficult to distinguish between Rayleigh fractionation and fluid mixing (Wilkinson et al. 2005). For example, although the fluid mixing has been alternatively proposed to explain the Zn isotopic variations of sphalerite from an Irish ore field, the dominant mechanism was preferentially attributed to Rayleigh fractionation (Wilkinson et al. 2005). Previous studies have demonstrated that Fe is preferentially precipitated during early stages under relatively high-temperature conditions, both experimentally (Seewald and Seyfried 1990) and in hydrothermal systems (Kelley et al. 2009; Liu et al. 2012). Conversely, Cd is inclined to substitute for Zn in sphalerite during late stages under relatively low-temperature conditions (Liu et al. 2012; He et al. 2016; Wen et al. 2016). Therefore, theoretically, the Fe and Cd concentrations of sphalerite should be decreasing and increasing respectively from the early to late stages during fluid evolution. Moreover, the trends toward higher δ^{66}Zn values in later precipitated sphalerite have been found to be mirrored by decreasing Fe concentration, which has been interpreted as Rayleigh fractionation (John et al. 2008; Kelley et al. 2009). Therefore, the variations of Fe and Cd concentrations in sphalerite can be used as additional proxies to identify the Rayleigh fractionation. However, during fluid mixing, the distributions of Fe and Cd contentions in sphalerite are dominated by multiple parameters (e.g., pH, temperature, species of Zn complex, and fluid components), not only the temperature-dependent Rayleigh fractionation (Fujii et al. 2011; Liu et al. 2012; Pašava et al. 2014; He et al. 2016; Wen et al. 2016). Therefore, during fluid mixing, the Fe and Cd concentrations in sphalerite could not change like the process of Rayleigh fractionation of a single fluid. For example, the decreasing Cd content in sphalerite from the early to late stages have also been reported from the Tianbaoshan and Daliangzi deposits in the SYG, which was interpreted as mixing of multi-source fluids based on geological and geochemical evidence (Liu et al. 2012; He et al. 2016). Therefore, the Fe and Cd concentrations in sphalerite could also be effective proxies to identify fluid mixing. If the Zn isotopic compositions of sphalerite are dominated by mixing of multi-source fluids, it would be feasible to trace the potential Zn sources of ore-forming fluids (Wilkinson et al. 2005).

In this study, the Zn and S isotopic compositions, and Fe and Cd concentrations of sphalerite from the Wusihe Zn–Pb deposit were investigated. The sphalerite samples were collected in a vertical direction from the well strata-bound orebodies at No. 12 adit in the Wusihe deposit. Sampling sphalerite ores from the bottom to the top of the orebodies allow us to distinguish the spatial evolution of Zn isotopic compositions of sphalerite. Combining with Fe and Cd concentrations, we would like to identify the mechanism that controls Zn isotopic variations of sphalerite in this deposit. Moreover, the new results allow us to trace the possible sources of ore-forming Zn and S in the Wusihe Zn–Pb deposit.

2 Geological setting

The SYG polymetallic mineralization province is tectonically located in the southwest margin of the Yangtze Craton (Fig. 1A). The SYG region is mainly composed of Mesoproterozoic folded basements, Ediacaran to Paleozoic marine sedimentary sequences, and Mesozoic to Cenozoic terrestrial sedimentary sequences (Liu and Lin 1999; Xiong et al. 2018). The folded basements include the Dongchuan, Kunyang, and Huili Groups that largely consist of phyllite, graywackes, dolostone, and volcanic rocks (Zhou et al. 2014b; Xiong et al. 2018). The Ediacaran to Paleozoic marine sedimentary sequences are composed of carbonates, black shales, clasolites, and widespread sulfate-bearing evaporate (Liu and Lin 1999; Zhou et al. 2014b). The Mesozoic to Cenozoic terrestrial sedimentary sequences are characterized by entirely continental origin (Liu and Lin 1999; Zhou et al. 2014b). The Ediacaran Dengying Formation (mainly dolostone) is the most important ore-hosting strata in the SYG area, which holds over 50% of

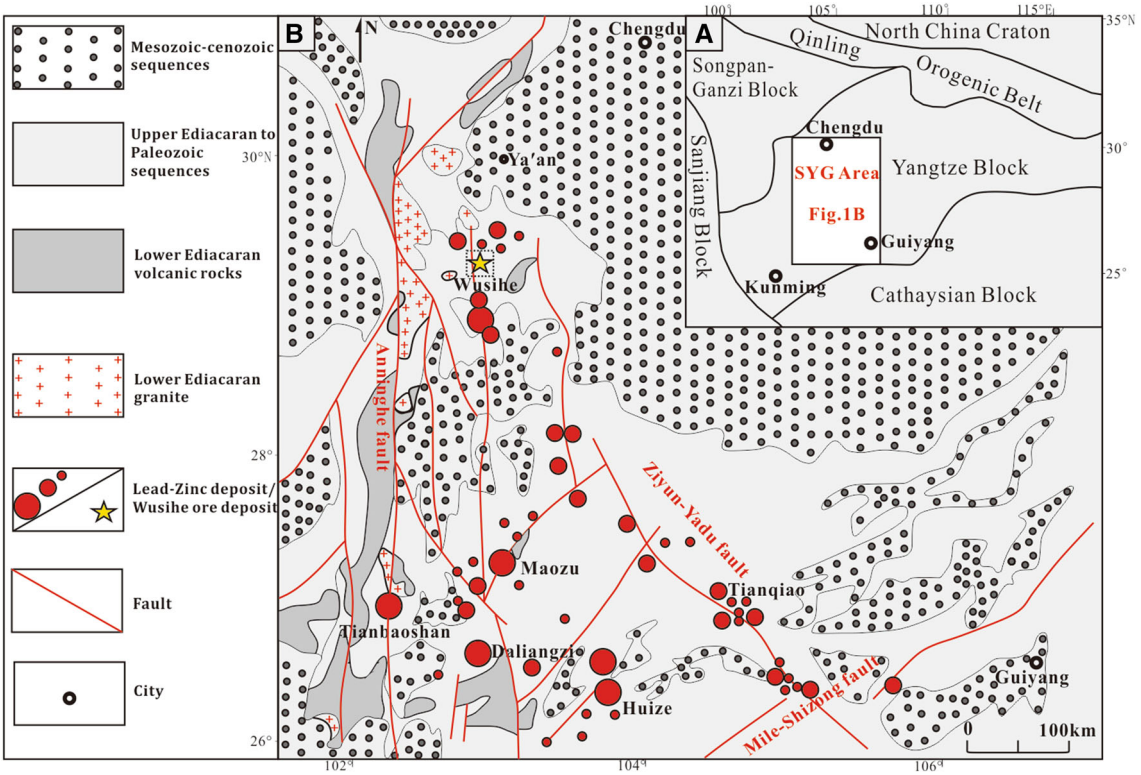

Fig. 1 Map of the tectonic framework of South China (**A**). Regional geological map of the Sichuan–Yunnan–Guizhou Zn–Pb metallogenic province, showing the distribution of major faults and Zn–Pb ore deposits (**B**) (modified from Xiong et al. 2016)

the regional Zn–Pb deposits (Luo et al. 2019). Tectonically, those deposits that occurred in the SYG are distributed in the triangular area enclosed by the Anninghe, Ziyun-Yadu, and Mile-Shizong regional fractures (Fig. 1B; Guan and Li 1999; Zhang et al. 2015). These regional fractures, which act as conduits for hydrothermal fluids, commonly control the migration of ore-forming fluids (Zhang et al. 2015; Xiong et al. 2018). And a series of thrust-folds are the primary ore-controlling and ore-hosting structures for the regional Zn–Pb mineralization (Zhang et al. 2015; Xiong et al. 2018). The primary magmatic activity in the SYG area is the Permian Emeishan flood basalts (~ 250 Ma; Zhou et al. 2002), which cover an area of over 250,000 km^2 and spatially coexist with the Zn–Pb deposits occurred in the SYG (Zhou et al. 2014a, b).

The Wusihe Zn–Pb deposit is located in the northern SYG in Ya'an city, Sichuan province (Fig. 1B). Within the Wusihe ore field, exposed strata mainly include the Ediacaran Dengying Formation and Cambrian to Permian marine sedimentary sequences (Fig. 2). The Wusihe Zn–Pb deposit is structurally controlled by the Wangmaoshan thrust-fault and the Wanlicun syncline (Fig. 2). The Wangmaoshan thrust-fault, crosscutting the Dengying Formation and the Lower Cambrian strata and dipping 65°–70° (Zheng 2012; Xiong et al. 2018), is the major ore-controlling fault in the mining area. The NS-trending Wanlicun syncline, including the Ediacaran and Paleozoic strata and plunging to the south, largely controls the distribution of the orebodies in the Wusihe deposit (Zheng 2012; Xiong et al. 2018). In the Wusihe Zn–Pb deposit, the main orebodies occurred in the Wanlicun syncline and were strata-bound within the Dengying Formation strata (Fig. 2). The Wusihe Zn–Pb deposit yields Zn–Pb resources of ~ 3.7 Mt at average grades of 12.50 wt.% Zn and 3.15 wt.% Pb (Zheng 2012). The ore minerals include sphalerite and galena, where the sphalerite is the primary economic mineral. The major gangue minerals are dolomite and quartz, also with minor pyrite and calcite. Sphalerite ores are characterized by disseminated, banded and veined structures (Fig. 3). The alteration type of the host rock principally includes silicification, pyritization, and dolomitization, which only occurred in local positions with a developed fissure (Zheng 2012).

The mineralization stages of the Wusihe deposit have been described in detail in the previous study (Xiong et al. 2018), where four stages were identified: Stage I is the pyrite stage (fine- to medium-grained pyrite disseminated within the dolomite), Stage II is the pyrite-pyrrhotite-galena-sphalerite-bitumen stage (most important economic mineralization stage), Stage III is the sphalerite-galena stage (subordinate economic stage), and Stage IV is the bitumen-calcite stage (final hydrothermal stage).

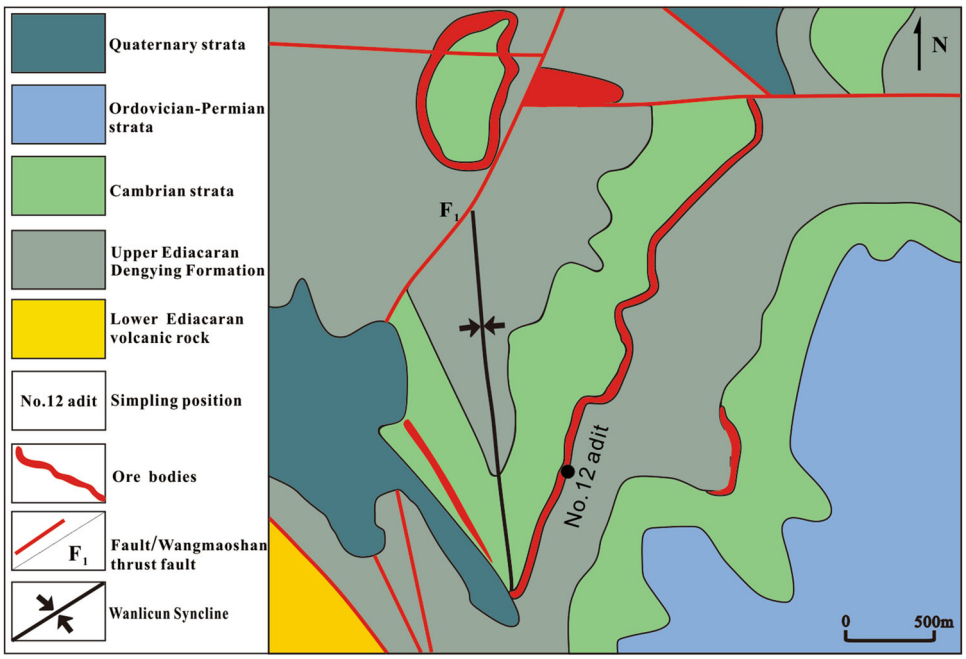

Fig. 2 Geological map of the Wusihe deposit, showing the major exposed strata, ore-controlling structures and sampling locations (modified from Lin 2005)

3 Sampling and analytical methods

3.1 Samples

Nine representative sphalerite samples were collected from the strata-bound orebodies in a vertical direction in No. 12 adit (Fig. 2). Three host rock samples were collected from the outcrop in the Wusihe ore field (N29.26°, E102.90°). All of these sulfide ores have a similar mineral assemblage, including sphalerite, galena, pyrite, and organic matter (Fig. 3). Sphalerite and galena are ubiquitous among all sulfide ores. Pyrite occurs in the wsh-12 and wsh-15. The organic matter is also common among these sulfide ores. The wsh-4, wsh-7, wsh-8 and wsh-10 were obtained from the bottom of the strata-bound orebodies in No. 12 adit, all with densely disseminated structure (Fig. 3A). The wsh-12 (Fig. 3B), wsh-14 (Fig. 3C) and wsh-15 (Fig. 3D) were collected from the middle position of the strata-bound orebodies in No. 12 adit, with sparsely disseminated, banded-disseminated, and veined structures, respectively. The wsh-16 (Fig. 3E) and wsh-17 (Fig. 3F) were sampled from the top of the strata-bound orebodies in No. 12 adit, with banded and veined structures, respectively. The separated sphalerite grains in the wsh-4, wsh-7, wsh-8, and wsh-10 samples were hand-picked under a binocular microscope. Other sphalerite samples for analysis were obtained by the Micro-Drill Sampling System (MSS) at the State Key Laboratory of Ore Deposit Geochemistry, Institute of Geochemistry, Chinese Academy of Sciences. The tungsten steel used in the MSS has a diameter of 0.5 mm, which can greatly avoid the contamination from host rocks.

3.2 Methods

Sphalerite and carbonate samples were digested by HNO_3 (15 mol/L) and HCl (6 mol/L), respectively, at 120 °C for 24 h. Sample solutions were evaporated to dryness and then were digested in 2 mL 2N HCl. The Zn was purified from the other matrix elements using anion exchange chromatography, as reported by Tang et al. (2006). Zinc isotope ratios and concentrations were measured using Nu Plasma MC-ICP-MS in a low-resolution mode at the State Key Laboratory of Ore Deposit Geochemistry, Institute of Geochemistry, Chinese Academy of Sciences. Mass discrimination effects were corrected using a combined sample-standard bracketing (SSB) (Li et al. 2008; Zhou et al. 2014a, b). Accuracy and reproducibility were assessed by replicate analyses of the international standards BHVO-2 (basalt), which yielded an average $\delta^{66}Zn$ value of 0.30 ± 0.04 ‰ (2σ, n = 6), consistent with previously reported values (Herzog et al. 2009; Liu et al. 2016). Each result is the mean value over the N number of repeats and all results are reported relative to the JMC Lyon Zn standard (Maréchal et al. 1999) based on the difference between the IRMM3702 and JMC Lyon Zn solution ($\Delta^{66}Zn_{IRMM3702\text{-}JMC\ Lyon}$ = 0.30 ‰; Moeller et al. 2012; Samanta et al. 2016).

Sulfur isotope analyses were carried out using a Thermo Flash 2000 at the State Key Laboratory of Resource Utilization and Environmental Restoration, Institute of

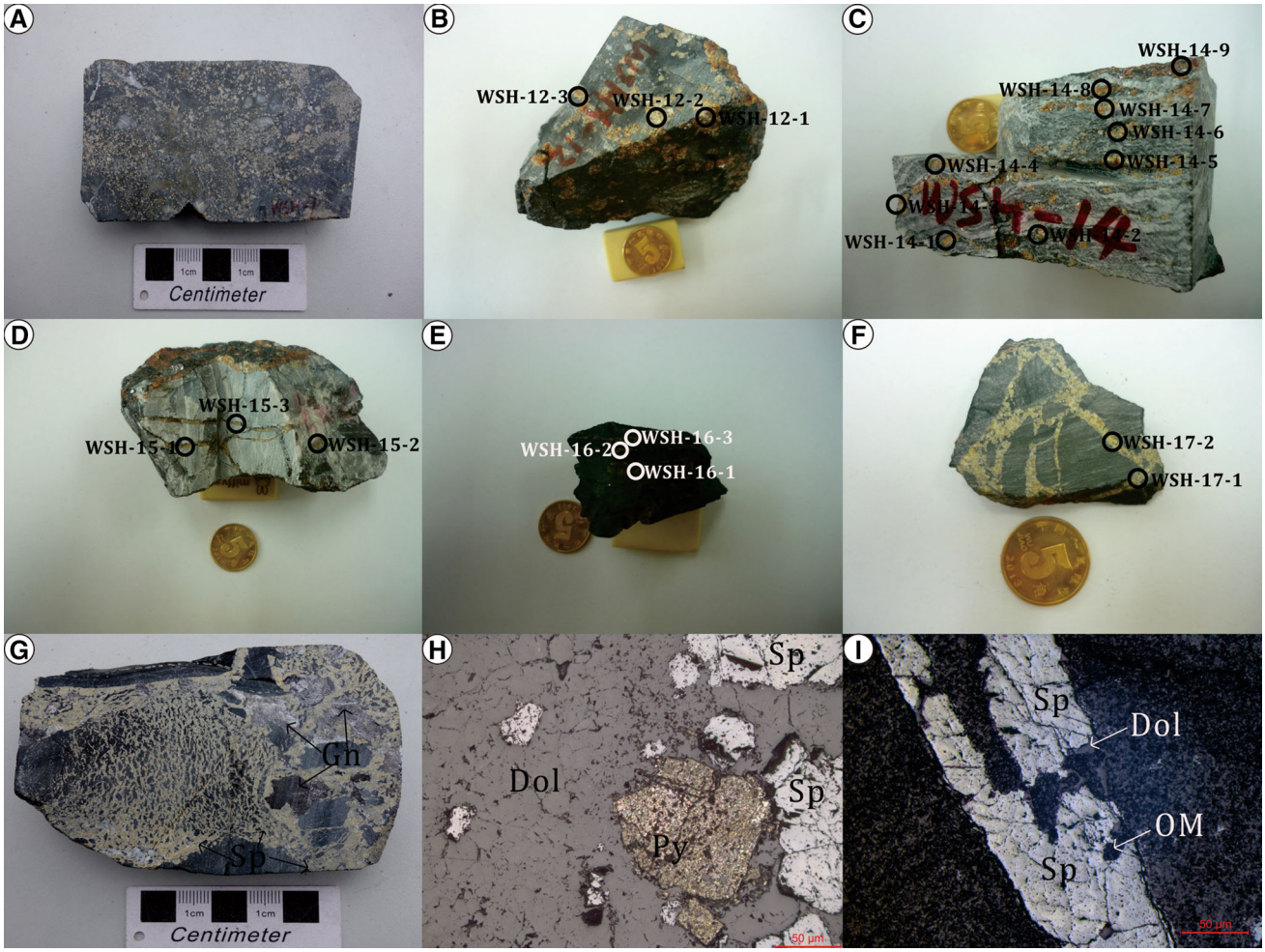

Fig. 3 The specimen photo of the bottom wsh-7 sample, showing the densely disseminated structure (**A**); the specimen pictures of the middle part wsh-12 (**B**), wsh-14 (**C**) and wsh-15 (**D**) samples, showing the micro-drilled positions, and sparsely disseminated, banded-disseminated and veined structures, respectively; The specimen photos of the top wsh-16 (**E**) and wsh-17 (**F**) samples, showing the micro-drilled positions, and banded and veined structures, respectively; the specimen photo and photomicrographs of main mineralization (**G**, **H** and **I**), *Gn* galena, *Dol* dolomite, *Sp* sphalerite, *Py* pyrite, *OM* organic matter

Geographic Science and Natural Resources Research, Chinese Academy of Sciences. IAEA-S-1 (Ag_2S; $\delta^{34}S_{CDT} = -0.3 \pm 0.2$ ‰, n = 6) were used as the external standards. The analysis errors (2σ) are better than 0.1 ‰ of the replication of standard materials. Sulfur isotopic compositions are reported relative to the Canyon Diablo Troilite (CDT).

The concentration of Fe and Cd of sphalerite were measured by the PinAAcle 900F atomic absorption spectrometer at the State Key Laboratory of Environmental Geochemistry, Institute of Geochemistry, Chinese Academy of Sciences. The Fe and Cd concentration of bulk-rock samples (host rocks) were measured by ICP-MS at ALS Chemex (Guangzhou) Co. Ltd. The relative analysis error of the Fe and Cd concentration is less than 5%. Moreover, we use the $Fe_{(ppm)}/Zn_{(\%)}$ and $Cd_{(ppm)}/Zn_{(\%)}$ to evaluate the Fe and Cd contents in sphalerite, which can diminish the interference of different proportion incorporation of host rocks.

4 Results

Zinc and sulfur isotopic compositions, and Fe and Cd concentrations of sphalerite from the Wusihe Zn–Pb deposit are shown in Table 1. The $\delta^{66}Zn$ values in sphalerite vary from 0.14 to 0.62 ‰ and yield an increasing trend from the bottom to the top of the well strata-bound orebodies in No. 12 adit (Fig. 4). The $\delta^{34}S$ values of sphalerite vary from 5.1 to 15.4 ‰ and also yield an increasing trend from the bottom to the top of the well strata-bound orebodies in No. 12 adit, which becomes more obvious when the wsh-14 sample is excluded (Fig. 5). In addition, the $\delta^{66}Zn$ and $\delta^{34}S$ values of sphalerite are

Table 1 The $\delta^{66}Zn$–$\delta^{34}S$ values and Zn–Fe–Cd contents in sphalerite samples, host rock samples, and basement samples

No.	Positions	Objects	Zn (wt.%)	Fe (wt.%)	Cd ($\times 10^{-6}$)	$\delta^{66}Zn$ (‰)	$\delta^{34}S$ (‰)
WSH-4	Bottom orebody	Sphalerite	–	0.12	5864	0.18 ± 0.05	10.5
WSH-7	Bottom orebody	Sphalerite	–	0.07	7202	0.14 ± 0.06	10.5
WSH-8	Bottom orebody	Sphalerite	–	0.14	3058	0.21 ± 0.02	11.6
WSH-10	Bottom orebody	Sphalerite	–	0.08	9214	0.19 ± 0.06	8.4
WSH-12-1	Middle orebody	Sphalerite ores	22.54	0.68	776	0.35 ± 0.02	13.4
WSH-12-2	Middle orebody	Sphalerite	49.02	1.25	1633	0.38 ± 0.03	12.7
WSH-12-3	Middle orebody	Sphalerite	46.54	0.83	1983	0.31 ± 0.03	12.8
WSH-14-1	Middle orebody	Sphalerite	51.52	1.81	985	0.38 ± 0.03	7.1
WSH-14-2	Middle orebody	Sphalerite	52.02	1.76	716	0.51 ± 0.06	7.4
WSH-14-3	Middle orebody	Sphalerite	46.98	1.18	1154	0.44 ± 0.01	5.1
WSH-14-4	Middle orebody	Sphalerite	47.46	7.50	622	0.44 ± 0.07	11.7
WSH-14-5	Middle orebody	Sphalerite	54.39	1.85	884	0.41 ± 0.05	13.3
WSH-14-6	Middle orebody	Sphalerite	48.72	2.03	607	0.50 ± 0.08	11.5
WSH-14-7	Middle orebody	Sphalerite	49.99	2.16	629	0.41 ± 0.07	12.6
WSH-14-8	Middle orebody	Sphalerite	47.02	1.74	802	0.52 ± 0.11	12.5
WSH-14-9	Middle orebody	Sphalerite	42.41	1.81	1062	0.41 ± 0.09	13.0
WSH-15-4	Middle orebody	Sphalerite	40.96	2.24	737	0.46 ± 0.08	14.1
WSH-15-5	Middle orebody	Sphalerite	49.39	2.68	711	0.38 ± 0.05	14.1
WSH-15-6	Middle orebody	Sphalerite	52.70	2.82	777	0.44 ± 0.06	13.1
WSH-16-1	Top orebody	Sphalerite	45.99	4.32	1056	0.44 ± 0.06	14.9
WSH-16-2	Top orebody	Sphalerite	40.87	4.14	1095	0.39 ± 0.01	15.4
WSH-16-3	Top orebody	Sphalerite ores	37.43	4.08	734	0.39 ± 0.05	15.0
WSH-17-3	Top orebody	Sphalerite	47.82	6.38	468	0.60 ± 0.05	14.1
WSH-17-4	Top orebody	Sphalerite	48.28	7.31	426	0.62 ± 0.06	14.5

No.	Positions	Host rocks	Zn (ppm)	$\delta^{66}Zn$ (‰)
WSH_{18}-5	Shallow ground	Carbonates	204	0.23 ± 0.04
WSH_{18}-8	Shallow ground	Carbonates	25	0.50 ± 0.01
WSH_{18}-16	Shallow ground	Carbonates	9	0.20 ± 0.01

No.	Positions	Basement rocks	Zn (ppm)	$\delta^{66}Zn$ (‰)
WC-1	Shallow ground	Carbonates	3	0.21 ± 0.04
HS-4	Shallow ground	Carbonates	24	0.10 ± 0.04
TBS_{16}-2	Shallow ground	Graywackes	61	0.30 ± 0.03
Td1900-8	Shallow ground	Phyllites	115	0.15 ± 0.05
Td1900-3	Shallow ground	Phyllites	199	0.34 ± 0.02

"–" mean not measured; the Zn concentration of the bottom sphalerites (hand-picked sphalerite separates) theoretically is ~ 67% considering their low Fe concentration; the data of the basement samples are collected from Zhang et al. (2019)

covariant in this deposit (Fig. 6). Three host rock samples contain Zn from 9 ppm to 204 ppm and yield $\delta^{66}Zn$ values from 0.20 to 0.50 ‰. Five basement samples contain Zn from 3 to 199 ppm and yield $\delta^{66}Zn$ values from 0.10 to 0.34 ‰.

5 Discussion

5.1 Possible mechanisms for Zn isotopic variations

The Zn isotopic compositions of sphalerite from the Wusihe Zn–Pb deposit range from 0.14 to 0.62 ‰ that increase from the bottom to the top of the well strata-bound orebodies (Fig. 4). The spatial evolution of Zn isotopic

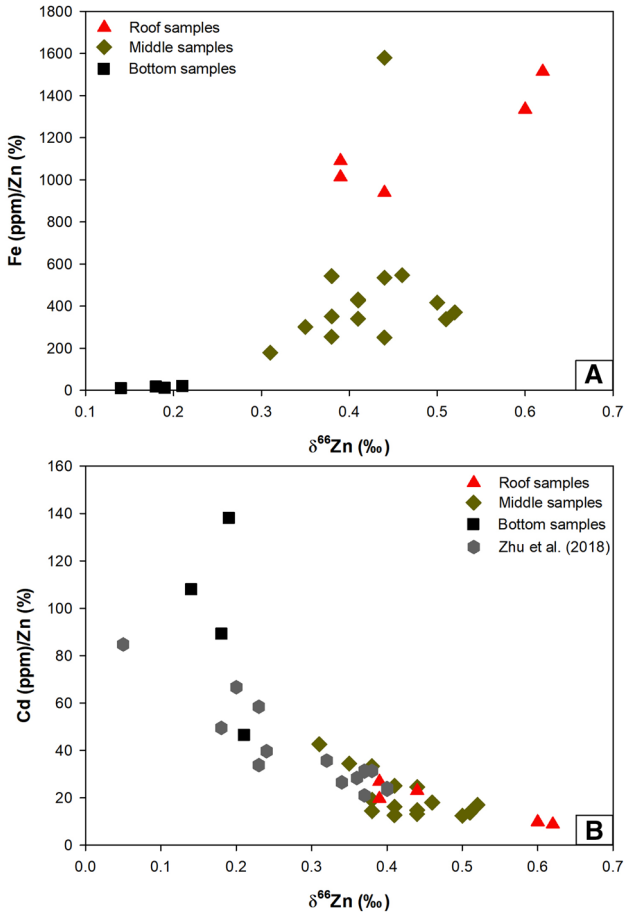

Fig. 4 The correlation between δ^{66}Zn and Fe (ppm)/Zn (%) values (**A**); the correlation between δ^{66}Zn and Cd (ppm)/Zn (%) values (**B**). Using the Fe (ppm)/Zn (%) and Cd (ppm)/Zn (%) values to evaluate the Fe and Cd contents in sphalerite can diminish the interference from different proportion incorporation of host rocks. The gray polygon data were cited from Zhu et al. (2018)

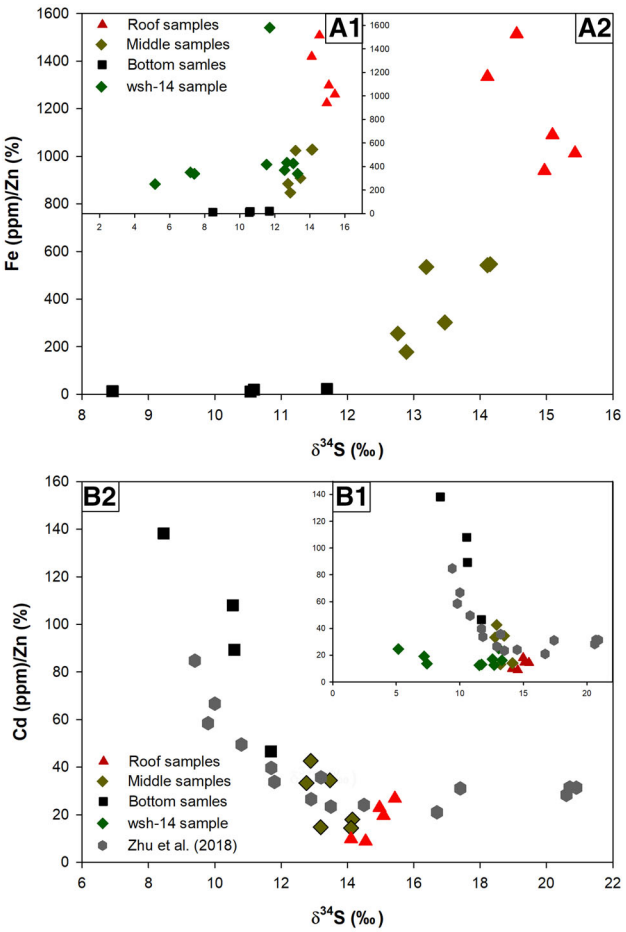

Fig. 5 The correlation between δ^{34}S and Fe (ppm)/Zn (%) values of all samples (**A**1), without the wsh-14 sample (**A**2); The correlation between δ^{34}S and Cd (ppm)/Zn (%) values of all samples (**B**1), without the wsh-14 sample (**B**2). The gray polygon data were cited from Zhu et al. (2018)

composition in hydrothermal system has been attributed to three potential mechanisms, including temperature variation, Rayleigh fractionation, and mixing of multi-source fluids (Mason et al. 2005; Wilkinson et al. 2005; Toutain et al. 2008; Kelley et al. 2009; Gagnevin et al. 2012; Pašava et al. 2014; Zhou et al. 2014a, b; Gao et al. 2017).

The potential influence of temperature gradients on Zn isotopic fractionation has been examined in previous studies, but their results obtained at different temperature conditions are not consistent. For example, the systematically increasing δ^{66}Zn values (− 0.03 to 0.23 ‰) away from the hydrothermal vent (~ 300 °C) in the Alexandrinka VMS deposit were ascribed to temperature-controlled variations (Mason et al. 2005). Furthermore, in the Merapi volcano system (590–297 °C), the Zn isotopic composition of high-temperature fumarolic gases (0.05–0.85 ‰) is much lower than that of their low-temperature condensates (1.48–1.68 ‰), which was also interpreted as temperature-dependent Rayleigh

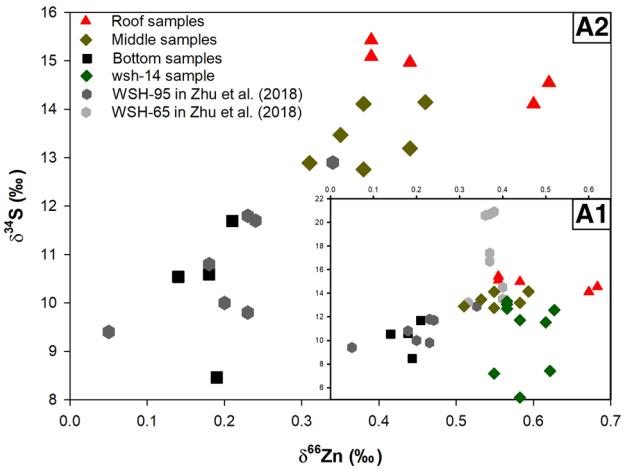

Fig. 6 The correlation between δ^{66}Zn and δ^{34}S values of all samples (**A**1), without the wsh-14 sample (**A**2). The gray polygon data were cited from Zhu et al. (2018)

fractionation (Toutain et al. 2008). However, several studies found that no correlation exists between the δ^{66}Zn values and temperatures when the temperatures were lower than 300 °C, either in an experiment (30 and 50 °C; Maréchal and Sheppard 2002) or in a hydrothermal system (60–250 °C; Wilkinson et al. 2005). These observations may indicate that the influence of temperature gradients on Zn isotope fractionation is negligible when the temperatures are lower than 300 °C. The homogenization temperatures of fluid inclusions in hydrothermal minerals from the Wusihe Zn–Pb deposit vary from 140 to 285 °C and mostly cluster between 150 and 250 °C (Lin 2005; Xiong et al. 2016). Therefore, it is suggested that temperature gradients could not dominate the Zn isotopic variations of sphalerite from the Wusihe Zn–Pb deposit.

Experiments demonstrated that early precipitated sulfides from the same solution are ^{64}Zn-enriched, whereas late precipitated sulfides are ^{66}Zn-enriched (Archer et al. 2004). Studies in hydrothermal systems have also confirmed that Rayleigh distillation could fractionate Zn isotopes between sphalerite and fluid, resulting in systematically increasing δ^{66}Zn values in sphalerite from the early to late stages (Wilkinson et al. 2005; Kelley et al. 2009; Gagnevin et al. 2012; Zhou et al. 2014a, b; Gao et al. 2017). Assuming that the systematically increasing δ^{66}Zn values of sphalerite from the Wusihe deposit were dominated by Rayleigh fractionation, it would indicate that, in a vertical direction, the bottom sphalerites precipitated earlier than the upper sphalerites. However, there is no evidence that the mineralization stages of this deposit are associated with the height positions of the well strata-bound orebodies. And these sulfide ores are similarly composed of sphalerite, galena, and minor pyrite (Fig. 3), which could indicate these sulfide ores formed from the same stage (stage II; Xiong et al. 2018). Moreover, Rayleigh fractionation model cannot explain the correlations of δ^{66}Zn values and Fe–Cd concentrations in sphalerite from this deposit. Previous studies have demonstrated that Fe is preferentially precipitated during early stages under relatively high-temperature conditions, both experimentally (Seewald and Seyfried 1990) and in hydrothermal systems (Kelley et al. 2009; Liu et al. 2012). Conversely, Cd is inclined to substitute for Zn in sphalerite during late stages under relatively low-temperature conditions (Liu et al. 2012; He et al. 2016; Wen et al. 2016). Assuming that Zn isotopic variations of sphalerite from the deposit are dominated by Rayleigh fractionation, there would be negative correlations between δ^{66}Zn values and Fe content and positive correlations between δ^{66}Zn values and Cd content in sphalerite. For example, during Rayleigh fractionation processes, higher δ^{66}Zn values in later precipitated sphalerite have been found to possess lower Fe concentration in natural hydrothermal systems (John et al. 2008; Kelley et al. 2009). In fact, the δ^{66}Zn values correlate with Fe positively and with Cd negatively in sphalerite from this deposit (Fig. 4). The clear correlations between δ^{66}Zn values and Fe and Cd contents in sphalerite indicate that their variations are dominated by a similar mechanism. Therefore, the Rayleigh fractionation could not be responsible for the spatial evolution in δ^{66}Zn values of sphalerite in the Wusihe deposit.

Similar to the Wusihe deposit, the decreasing Cd content in sphalerite from the early to late stages have also been reported from the Tianbaoshan and Daliangzi Zn–Pb deposits in the SYG, which was interpreted as mixing of multi-source fluids based on geological and geochemical evidence (Liu et al. 2012; He et al. 2016). The mixing of multi-source fluids could also result in a spatial evolution in δ^{66}Zn values of sphalerite on a deposit scale (Wilkinson et al. 2005). The Emeishan basalts, basements and host rocks are three potential sources for the regional Zn–Pb mineralization in the SYG (Huang et al. 2003; Han et al. 2007; Ye et al. 2011; Zhou et al. 2014b, 2018; Zhu et al. 2016; Xiong et al. 2018). Recently, the ore-forming age of the Wusihe deposit has been constrained to 411 ± 10 Ma via the Rb–Sr isochron (Xiong et al. 2018), and thus the much younger Emeishan basalts (~ 250 Ma; Zhou et al. 2002) are impossible to contribute to the mineralization of the Wusihe Zn–Pb deposit. Five basement samples, including carbonates, graywackes, and phyllites, yield low δ^{66}Zn values from 0.10 to 0.34 ‰, similar to the Zn isotopic signals documented in the bottom sphalerite samples of the well strata-bound orebodies in this deposit. Moreover, the basements of an Irish orefield, where the rock assemblage is similar to here (mainly graywackes and volcanic rocks), also have been reported to have low Zn isotopic signatures (0.00–0.18 ‰; Wilkinson et al. 2005; Gagnevin et al. 2012). On the other hand, three carbonate samples collected from the host rocks yield higher δ^{66}Zn values of 0.20–0.50 ‰, similar to the Zn isotopic signatures recorded in the upper sphalerites of the well strata-bound orebodies in this deposit. Furthermore, biogenic carbonates have been studied with heavy Zn isotopic compositions (mean = 0.91 ‰; Pichat et al. 2003). Combining with the fact that the biogenic carbonates are widespread in the host rocks (Feng et al. 2009; He et al. 2016), the host rock-derived fluid could have higher Zn isotopic signature than that of basement-derived fluid. Therefore, the spatial variation in δ^{66}Zn values of sphalerite from the Wusihe Zn–Pb deposit could result from mixing basement-derived fluid of lighter Zn isotopic composition with host rock-derived fluid of heavier Zn isotopic composition (Figs. 4 and 7).

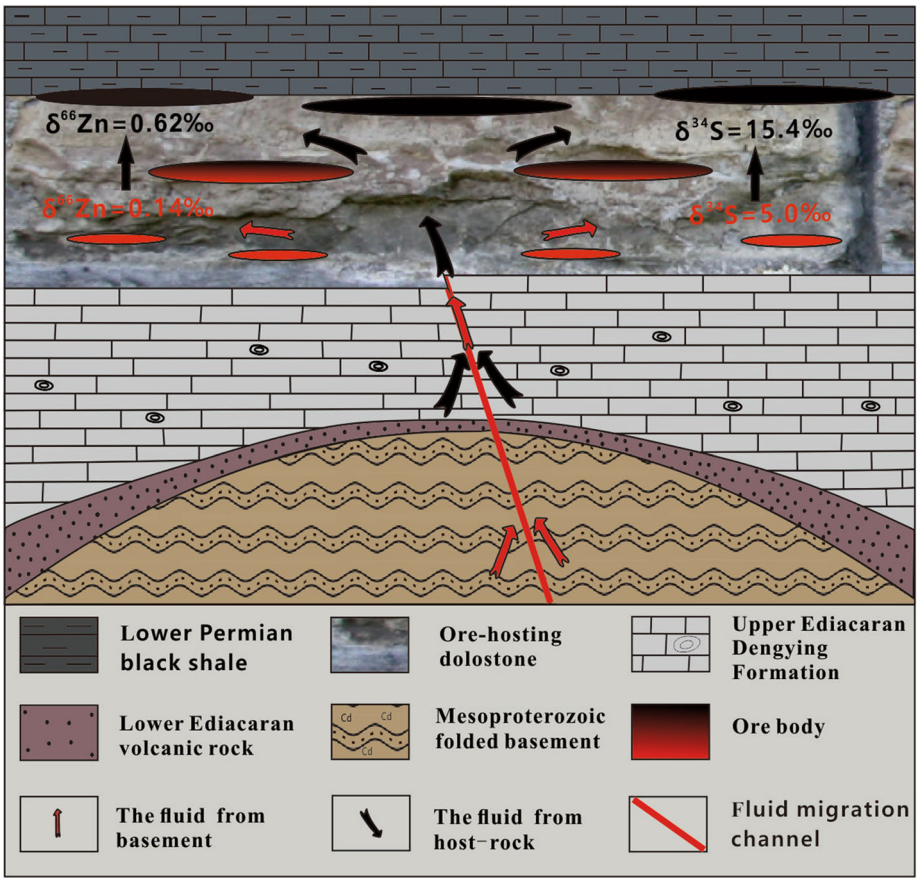

Fig. 7 Mixing model sketch of the Wusihe ore deposit. The mixing occurred under the black shales; the fluid from host rocks yields higher $\delta^{66}Zn$ and $\delta^{34}S$ values, whereas the fluid from folded basements yields lower $\delta^{66}Zn$ and $\delta^{34}S$ values

5.2 Possible mechanisms for sulfur isotopic variation

The sulfur isotopic compositions of sphalerite from the Wusihe Zn–Pb deposit vary from 5.1 to 15.4 ‰ (mean = 12.1 ‰; Fig. 6), consistent with the previous study where the $\delta^{34}S$ values of sulfide were reported to range from 7.1 to +15.5 ‰ (mean = 11.4 ‰; Xiong et al. 2018). In the Wusihe Zn–Pb deposit, an increasing trend in $\delta^{34}S$ values from the bottom to the top of the well strata-bound orebodies also exists, which becomes more obvious when the wsh-14 sample is excluded (Fig. 5). The increasing $\delta^{34}S$ values in sulfide could be alternatively attributed to kinetic fractionation from single hydrothermal fluid due to fluid cooling (Rye and Ohmoto 1974; Böttcher et al. 1998; Gagnevin et al. 2012; Zhu et al. 2017). Similar to the $\delta^{66}Zn$ values in the deposit, the $\delta^{34}S$ values also correlate with Fe positively and with Cd negatively in sphalerite (Fig. 4), which cannot be attributed to kinetic fractionation (Bethke and Borton 1971; Liu et al. 2012; Belissont et al. 2014; He et al. 2016; Wen et al. 2016). As so, the kinetic fractionation could not be responsible for the sulfur isotopic variation of sphalerite in the Wusihe Zn–Pb deposit.

Previous studies also demonstrated that the temporally and spatially dependent $\delta^{34}S$ values could be interpreted as mixing multi-source fluids (Rye and Ohmoto 1974; Bortnikov et al. 1995; Gagnevin et al. 2012; Thiessen et al. 2016; Zhu et al. 2017). The Emeishan basalts, basements, and host rocks are three potential sulfur sources for the regional Zn–Pb mineralization in the SYG (Huang et al. 2003; Han et al. 2007; Ye et al. 2011; Zhou et al. 2014b, 2018; Zhu et al. 2016; Xiong et al. 2018). The $\delta^{34}S$ values of sphalerite from the Wusihe Zn–Pb deposit range from 5.1 to 15.4 ‰ (mean = 12.1 ‰; Fig. 6), significantly different from mantle-derived magmatic sulfur (~ 0 ‰; Chaussidon et al. 1989), and thus that the magma-derived (Emeishan basalts) sulfur is ruled out. In the SYG, S-bearing evaporates are widespread in the host rocks, the sulfur isotopic compositions of these evaporates have been reported to range from 20.0 to 38.7 ‰ (mean = 29.0 ‰; Zhang et al. 2004; Xiong et al. 2016). The homogenization temperatures of the ore-forming fluids in the deposit yield an average value of 197 °C (n = 47; Lin 2005), suggesting ~ 10 ‰ sulfur isotopic fractionation between sulfides and sulfates (200 °C, $\Delta^{34}S_{sulfate-sulfide}$ = 10 ‰; Machel et al. 1995). However, in the Wusihe deposit, the mean sulfur isotopic composition of sulfides is ~ 12.0 ‰ (here; Xiong et al. 2018), which is ~ 17 ‰ lower than that of evaporates (29.0 ‰). It is suggested, thus, that there could be another sulfur source providing lighter sulfur isotopes than

evaporates for the Wusihe deposit. The much lighter sulfur isotopic compositions of sulfide have been reported from the Tianbaoshan deposit in the SYG (0.2–5.0 ‰), which has been constrained to basement-derived sulfur after precluding the possibility from host rocks and mantle magma (Zhu et al. 2016). Therefore, the basements could be another potential sulfur source supplying lighter sulfur isotopes than evaporates for the Wusihe deposit. As so, similar to Zn isotopic system in the deposit, mixing of the ore-forming fluids from basement rocks and host rocks, respectively, could dominate the spatial variation in $\delta^{34}S$ values of sphalerite from the Wusihe Zn–Pb deposit (Figs. 5 and 7).

If it is the case, the mixing model may suggest an explanation to the sulfur isotopic outliers in the wsh-14 sample collected from the middle part of the well strata-bound orebodies (Fig. 3C). For the other hand specimens, $\delta^{34}S$ values of micro-drilled sphalerite samples within the same specimen only slightly change, without exceeding 1.0 ‰, which suggests that these hand specimens could only record the homogeneous sulfur isotopic signature of a single fluid. However, the sulfur isotopic variation of the wsh-14 sample (5.16–13.05 ‰), with nine micro-drilled samples, almost covers the entire range of that of all the sphalerite samples from the deposit (5.16–15.43 ‰). Note that the wsh-14 sample was collected from the middle part of the well strata-bound orebodies, which may be a right position for fluid mixing. Here, we ascribe the largely varying $\delta^{34}S$ values in the wsh-14 sample to a localized heterogeneous mixing of two-source fluids and thus that the wsh-14 sample could document the sulfur isotopic characters of both the basements-derived fluid and host rock-derived fluid.

5.3 Implications from Zn and S isotopes

Previous studies have different opinions on the origin and mechanism of the Wusihe deposit. Lin (2005) and Zhu et al. (2018) argued that ore-forming components of the Wusihe deposit had been sourced from SEDEX hydrothermal systems, namely from the Mesoproterozoic basements. However, Xiong et al. (2018) demonstrated that the Wusihe deposit belongs to MVT deposit, and further proposed that Pb and Sr have been sourced from both host and basement rocks.

In this contribution, both independent Zn and S isotopic systems indicate that there is a fluid mixing from both host and basement rocks (Fig. 7), which is consistent with the inferences by Xiong et al. (2018). The fluid from the host rocks yields higher $\delta^{66}Zn$ and $\delta^{34}S$ values, whereas the fluid from the basement rocks yields lower $\delta^{66}Zn$ and $\delta^{34}S$ values. Moreover, the previous study demonstrated that mixing of two-source fluids with contrasting zinc and sulfur isotopic composition would induce covariant $\delta^{66}Zn$ and $\delta^{34}S$ values in sphalerite at a deposit scale (Wilkinson et al. 2005). The covariant $\delta^{66}Zn$ and $\delta^{34}S$ values in sphalerite are indeed observed in the Wusihe deposit (Fig. 6), which further validates the existence of fluid mixing. The mineralization deposition could happen when two source fluids mixed together below a black shale layer (Fig. 7), associating the changes in physical and chemical conditions of ore-forming fluids. The spatial variation in $\delta^{66}Zn$ and $\delta^{34}S$ values could be ascribed that the rock-derived brine migrated to the mineralization position earlier and inclined to fill stratigraphically higher spaces owing to fluid-pressure, while the subsequent basement-derived metamorphic fluids mainly migrated to stratigraphically lower position owing to limited spaces left.

6 Conclusion

In this contribution, Zn and S isotopes combined with Fe and Cd concentrations of sphalerite from the Wusihe Zn–Pb deposit in the SYG, Southwest China, have been examined. The results allow us to draw three conclusions as follows:

1. The spatial variation of $\delta^{66}Zn$ and $\delta^{34}S$ values of sphalerite from the Wusihe deposit resulted from the mixing of two-source fluids with contrasting Zn and S isotopic composition.
2. The fluid from the host rocks yields higher $\delta^{66}Zn$ ($\sim$ 0.6 ‰) and $\delta^{34}S$ values ($\sim$ 15 ‰), whereas the fluid from the basement rocks yields lower $\delta^{66}Zn$ ($\sim$ 0.2 ‰) and $\delta^{34}S$ values ($\sim$ 5 ‰).
3. The covariant isotopic compositions of Zn and S could be an effective proxy in reflecting fluids mixture, in which the Zn and S were transported together.

Acknowledgements This project was funded by the Strategic Priority Research Program (B) of the Chinese Academy of Sciences (XDB18030302), the National Key R&D Program of China (2017YFC0602503), the National Natural Science Foundation of China (U1812402, 41430315, 41573011, 41625006). We give thanks to the two reviewers for reviewing the manuscript and the editor for providing comments and editorial reversions.

Compliance with ethical standards

Conflict of interest The authors declare that they have no conflicts of interest.

References

Archer C, Vance D, Butler I (2004) Abiotic Zn isotope fractionations associated with ZnS precipitation. Geochim Cosmochim Acta 68:A325

Belissont R, Boiron MC, Luais B, Cathelineau M (2014) LA-ICP-MS analyses of minor and trace elements and bulk Ge isotopes in zoned Ge-rich sphalerites from the Noailhac–Saint–Salvy deposit (France): insights on incorporation mechanisms and ore deposition processes. Geochim Cosmochim Acta 126:518–540

Bethke PH, Borton PB (1971) Distribution of some minor elements between coexisting sulfide minerals. Econ Geol 66:140–165

Bortnikov NS, Dobrovol'skaya MG, Genkin AD, Naumov VB, Shapenko VV (1995) Sphalerite-galena geothermometers: distribution of cadmium, manganese, and the fractionation of sulfur isotopes. Econ Geol 90:155–180

Böttcher ME, Smock AM, Cypionka H (1998) Sulfur isotope fractionation during experimental precipitation of iron (II) and manganese (II) sulfide at room temperature. Chem Geol 146:127–134

Chaussidon M, Albarède F, Sheppard SMF (1989) Sulphur isotope variations in the mantle from ion microprobe analyses of micro-sulphide inclusions. Earth Planet Sci Lett 92:144–156

Feng JQ, Li Y, Liu WZ (2009) Geological features and ore control conditions for the Tianbaoshan Zn–Pb deposit in Huili. Acta Geologica Sichuan 29(4):426–430 **(In Chinese with English abstract)**

Fujii T, Moynier F, Pons ML, Albarède F (2011) The origin of Zn isotope fractionation in sulfides. Geochim Cosmochim Acta 75(23):7632–7643

Gagnevin D, Boyce AJ, Barrie CD, Menuge JF, Blakeman RJ (2012) Zn, Fe and S isotope fractionation in a large hydrothermal system. Geochim Cosmochim Acta 88:183–198

Gao ZF, Zhu XK, Sun J, Luo ZH, Bao C, Tang C, Ma JX (2017) Spatial evolution of Zn–Fe–Pb isotopes of sphalerite within a single ore body: a case study from the Dongshengmiao ore deposit, Inner Mongolia, China. Miner Deposita 15:1–11

Guan SP, Li ZX (1999) Lead-sulfur isotope study of carbonate-hosted lead-zinc deposits at the eastern margin of the Kangdian axis. Geol Geochem 27:45–54 **(In Chinese with English abstract)**

Han RS, Liu CQ, Huang ZL, Chen J, Ma DY, Lei L, Ma GS (2007) Geological features and origin of the Huize carbonate-hosted Zn–Pb–(Ag) district, Yunnan, South China. Ore Geol Rev 31:360–383

He CZ, Xiao CY, Wen HJ, Zhou T, Zhu CW, Fan HF (2016) Zn–S isotopic compositions of the Tianbaoshan carbonate-hosted Zn–Pb deposit in Sichuan, China: implications for source of ore components. Acta Petrol Sin 32:3394–3406 **(In Chinese with English abstract)**

Herzog GF, Moynier F, Albarede F, Berezhnoy AA (2009) Isotopic and elemental abundances of copper and zinc in lunar samples, Zagami, Pele's hairs, and a terrestrial basalt. Geochim Cosmochim Acta 73:5884–5904

Hu RZ, Fu SL, Huang Y, Zhou MY, Fu SH, Zhao CH, Wang YJ, Bi XW, Xiao JF (2017) The giant South China Mesozoic low-temperature metallogenic domain: reviews and a new geodynamic model. J Asian Earth Sci 137:9–34

Huang ZL, Li WB, Chen J, Han RS, Liu CQ, Xu C, Guan T (2003) Carbon and oxygen isotope constraints on the mantle fluids join the mineralization of the Huize superlarge Pb–Zn deposits, Yunnan Province, China. J Geochem Explor 78(79):637–642

John SG, Rouxel OJ, Craddock PR, Engwall AM, Boyle EA (2008) Zinc stable isotopes in seafloor hydrothermal vent fluids and chimneys. Earth Planet Sci Lett 269:17–28

Kelley KD, Wilkinson JJ, Chapman JB, Crowther HL, Weiss DJ (2009) Zinc isotopes in sphalerite from base metal deposits on the red dog district, northern Alaska. Econ Geol 104:767–773

Li SZ, Zhu XK, Tang SH, He XX, Cai JJ (2008) The application of MC-ICP-MS to high-precision measurement of Zn isotope ratios. Acta Petrol Mineral 27:273–278 **(In Chinese with English abstract)**

Lin FC (2005) Hydrothermal exhalative metallogeny of stratiform Zn–Pb deposits on western margin of the Yangtze craton. Ph.D. Dissertation, Chengdu University of Technology, Chengdu, pp 1–113 (in Chinese with English abstract)

Liu HC, Lin WD (1999) Study on the law of Zn–Pb–Ag Ore deposit in northeast Yunnan. China. Yunnan University Press, Kunming, pp 1–468 **(in Chinese)**

Liu TG, Ye L, Zhou JX, Shao SX (2012) The correlativity of mineralization stages and Cd, Fe contents in the sphalerite. Bull Mineral Petrol Geochem 31:79–81 **(In Chinese with English abstract)**

Liu SA, Wang ZZ, Li SG, Huang J, Yang W (2016) Zinc isotope evidence for a large-scale carbonated mantle beneath eastern China. Earth Planet Sci Lett 444:169–178

Luo K, Zhou JX, Huang ZL, Wang XC, Wilde SA, Zhou W, Tian LY (2019) New insights into the origin of early Cambrian carbonate-hosted Pb–Zn deposits in South China: a case study of the Maliping Pb–Zn deposit. Gondwana Res 70:88–103

Machel HG, Krouse HR, Sassen R (1995) Products and distinguishing criteria of bacterial and thermochemical sulfate reduction. Appl Geochem 10:373–389

Maréchal CN, Sheppard SMF (2002) Isotopic fractionation of Cu and Zn between chloride and nitrate solutions and malachite or smithsonite at 30 degrees and 50 degrees C. In: Goldschmidt conference. Geochim Cosmochim Acta 66:A484

Maréchal CN, Télouk P, Albarède F (1999) Precise analysis of copper and zinc isotopic compositions by plasma-source mass spectrometry. Chem Geol 156(1–4):251–273

Mason TFD, Weiss DJ, Chapman JB, Wilkinson JJ, Tessalina SG, Spiro B, Horstwood MSA, Spratt J, Coles BJ (2005) Zn and Cu isotopic variability in the Alexandrinka volcanic-hosted massive sulphide (VHMS) ore deposit, Urals, Russia. Chem Geol 221(3–4):170–187

Moeller K, Schoenberg R, Pedersen RB, Weiss D, Dong SF (2012) Calibration of the new certified reference materials ERM-AE633 and ERM-AE647 for copper and IRMM-3702 for zinc isotope amount ratio determinations. Geostand Geoanal Res 36(2):177–199

Pašava J, Tornos F, Chrastný V (2014) Zinc and sulfur isotope variation in sphalerite from carbonate-hosted zinc deposits, Cantabria, Spain. Miner Deposita 49:797–807

Pichat S, Douchet C, Albarède F (2003) Zinc isotope variations in deep-sea carbonates from the eastern equatorial Pacific over the last 175 ka. Earth Planet Sci Lett 210(1–2):167–178

Rye RO, Ohmoto H (1974) Sulfur and carbon isotopes and ore genesis: a review. Econ Geol 69:826–842

Samanta M, Ellwood MJ, Mortimer GE (2016) A method for determining the isotopic composition of dissolved zinc in seawater by MC-ICP-MS with ^{67}Zn–^{68}Zn double spike. Microchem J 126:530–537

Seewald JS, Seyfried WE (1990) The effect of temperature on metal mobility in subseafloor hydrothermal systems: constraints from basalt alteration experiments. Earth Planet Sci Lett 101:388–403

Tang SH, Zhu XK, Cai JJ, Li SZ, He XX, Wang JH (2006) Chromatographic separation of Cu, Fe and Zn using AGMP-1 anion exchange resin for isotope determination by MC-ICP-MS. Rock Miner Anal 25:5–8 **(In Chinese with English abstract)**

Thiessen EJ, Gleeson SA, Bennett V, Creaser RA (2016) The Tiger deposit: a carbonate-hosted, magmatic-hydrothermal gold deposit, Central Yukon, Canada. Econ Geol 111:421–446

Toutain JP, Sonke J, Munoz M, Nonell A, Polvé M, Viers J, Freydier R, Sortino F, Joron JL, Sumarti S (2008) Evidence for Zn isotopic fractionation at Merapi Volcano. Chem Geol 253(1–2):74–82

Wang H, Sun ZJ, Cheng XY, Jiang BB (2016) The geochemical characteristics and metallogenic mechanism of the Daliangzi Pb-Zn deposit in Sichuan province. Acta Geol Sin (Engl Ed) 89:287–288

Wen HJ, Zhu CW, Zhang YX, Cloque C, Fan HF, Fu SH (2016) Zn/Cd ratios and cadmium isotope evidence for the classification of lead-zinc deposits. Sci Rep 20:5–8. https://doi.org/10.1038/srep25273

Wilkinson JJ, Weiss DJ, Mason TFD, Coles BJ (2005) Zinc isotope variation in hydrothermal systems: preliminary evidence from the Irish midlands ore field. Econ Geol 100(3):583–590

Xiong SF, Yao SZ, Gong YJ, Tan MT, Zeng GP, Wang W (2016) Ore-forming fluid and thermochemical sulfate reduction in the Wusihe lead-zinc deposit, Sichuan Province, China. Earth Sci 41:105–120 **(In Chinese with English abstract)**

Xiong SF, Gong YJ, Jiang SY, Zhang XJ, Li Q, Zeng GP (2018) Ore genesis of the Wusihe carbonate-hosted Zn–Pb deposit in the Dadu River Valley district, Yangtze Block, SW China. Miner Deposita 53(7):967–979

Ye L, Cook NJ, Ciobanu CL, Liu YP, Zhang Q, Liu TG, Gao W, Yang YL, Danyushevsky L (2011) Trace and minor elements in sphalerite from base metal deposits in South China: a LA-ICPMS study. Ore Geol Rev 39:188–217

Zhang TG, Chu XL, Zhang QR, Feng LJ, Huo WG (2004) The sulfur and carbon isotopic records in carbonates of the Dengying Formation in the Yangtze Platform, China. Acta Petrol Sin 20:717–724 **(in Chinese with English abstract)**

Zhang CQ, Wu Y, Hou L, Mao JW (2015) Geodynamic setting of mineralization of Mississippi Valley-type deposits in world-class Sichuan-Yunnan-Guizhou Zn–Pb triangle, southwest China: implications from age-dating studies in the past decade and the Sm–Nd age of Jinshachang deposit. J Asian Earth Sci 103:103–114

Zhang HJ, Xiao CY, Wen HJ, Zhu XK, Ye L, Huang ZL, Fan HF (2019) Homogeneous Zn isotopic compositions in the Maozu Zn–Pb ore deposit in Yunnan Province, Southwestern China. Ore Geol Rev 109:1–10

Zheng XZ (2012) Geological features and genesis of WuSiHe Zn–Pb deposit, Sichuan. M.Sc. Thesis, Chang'an University, Xi'an, pp 1–75 (in Chinese with English abstract)

Zhou MF, Malpas J, Song XY, Robinson PT, Sun M, Kennedy AK, Lesher CM, Keays RR (2002) A temporal link between the Emeishan large igneous province (SW China) and the end-Guadalupian mass extinction. Earth Planet Sci Lett 196:113–122

Zhou JX, Huang ZL, Yan ZF (2013) The origin of the Maozu carbonate-hosted Zn–Pb deposit, southwest China: constrained by C–O–S–Pb isotopic compositions and Sm-Nd isotopic age. J Asian Earth Sci 73:39–47

Zhou JX, Huang ZL, Zhou MF, Zhu XK, Gao JG, Mirnejad H (2014a) Geology, isotope geochemistry and ore genesis of the Shanshulin carbonate-hosted Zn–Pb deposit, Southwest China. Ore Geol Rev 63:209–225

Zhou JX, Huang ZL, Zhou MF, Zhu XK, Muchez P (2014b) Zinc, sulfur and lead isotopic variations in carbonate-hosted Pb–Zn sulfide deposits, southwest China. Ore Geol Rev 58:41–54

Zhou JX, Xiang ZZ, Zhou MF, Feng YX, Luo K, Huang ZL, Wu T (2018) The giant upper Yangtze Zn–Pb province in SW China: reviews, new advances and a new genetic model. J Asian Earth Sci 154:280–315

Zhu CW, Wen HJ, Zhang YX, Fan HF (2016) Cadmium and sulfur isotopic compositions of the Tianbaoshan Zn–Pb–Cd deposit, Sichuan Province, China. Ore Geol Rev 76:152–162

Zhu CW, Wen HJ, Zhang YX, Fu SH, Fan HF, Cloquet C (2017) Cadmium isotope fractionation in the Fule Mississippi Valley-type deposit, Southwest China. Miner Deposita 52:675–686

Zhu CW, Liao SL, Wang W, Zhang YX, Yang T, Fan HF, Wen HJ (2018) Variations in Zn and S isotope chemistry of sedimentary sphalerite, Wusihe Zn–Pb deposit, Sichuan Province, China. Ore Geol Rev 95:639–648